

## PHOTODEGRADATION STUDY OF THE FENVALERATE INSECTICIDE BY $^1\text{H}$ NMR, $^{13}\text{C}$ NMR, AND GC-MS AND STRUCTURAL ELUCIDATION OF ITS TRANSFORMATION PRODUCTS<sup>1</sup>

Diène Diégane Thiaré<sup>1,2\*</sup>, Pape Abdoulaye Diaw<sup>1,3</sup>, Olivier Maurice Aly Mbaye<sup>1</sup>, Diégane Sarr<sup>1,3</sup>, Mame Diabou Gaye-Seye<sup>1</sup>, Steven Ruellan<sup>2</sup>, Philippe Giamarchi<sup>4</sup>, François Delattre<sup>2</sup>, Atanasse Coly<sup>1</sup>, Jean-Jacques Aaron<sup>5\*</sup>

<sup>1</sup> Laboratoire de Photochimie et d'Analyse (LPA), Faculté des Sciences et Techniques, Université Cheikh Anta Diop, BP 5005, Dakar, Sénégal

<sup>2</sup> Unité de Chimie Environnementale et Interactions sur le Vivant (UCEIV), ULCO, BP 59140, Dunkerque, France

<sup>3</sup> Laboratoire Matériaux, Electrochimie et Photochimie Analytique, Université Alioune Diop, Bambey, Sénégal

<sup>4</sup> Laboratoire d'Optique et de Magnétisme (OPTIMAG), Université de Bretagne Occidentale (UBO), 6 Av. Victor Le Gorgeu, 29285, Brest Cedex, France

<sup>5</sup> Laboratoire Géomatériaux et Environnement (LGE), EA 4508, Université Paris-Est Marne-la-Vallée, 5 Boulevard Descartes, 77454, Marne-La-Vallée, France

jeanjacquesaaron@yahoo.fr

The photolysis of fenvalerate, a pyrethroid insecticide, was studied in acetonitrile by  $^1\text{H}$  nuclear magnetic resonance (NMR) and  $^{13}\text{C}$  NMR to identify the site of bond cleavage and gas chromatography-mass spectrometry (GC-MS) to establish the chemical structure of fenvalerate photoproducts. Ultraviolet (UV) irradiation of fenvalerate solutions was performed for 18 h with a solar light simulator, and the photolysis reaction obeyed first-order kinetics. Photolysis half-life time ( $t_{1/2}$ ) values ranged between 15.25 and 21.63 h (mean photodegradation percentage = 51.7 %) for  $^1\text{H}$  NMR and between 4.55 and 8.06 h (mean photodegradation percentage > 80 %) for  $^{13}\text{C}$  NMR. We observed five sites of bond cleavage, namely carbonyl-tertiary carbon, tertiary carbon-tertiary carbon, carbonyl-oxygen, carboxyl-tertiary carbon, and aromatic carbon-tertiary carbon, yielding photoproducts formation. GC-MS was associated with  $^1\text{H}$  NMR and  $^{13}\text{C}$  NMR to obtain a complete photodegradation mechanism. Before UV irradiation, two chromatogram peaks were obtained, due to the two fenvalerate isomers. Under irradiation, both peaks decreased, and new peaks appeared, corresponding to photoproduct formation. After a 12- to 13-h irradiation, 99.39 % of fenvalerate was degraded with a mean rate constant of  $0.305\text{ h}^{-1}$ . The chemical structure of the formed photoproducts was identified, either by using the National Institute of Standards and Technology (NIST) mass spectral database or by interpreting the mass spectra. Finally, a detailed mechanism was proposed for fenvalerate photodegradation.

**Keywords:** fenvalerate, insecticide;  $^1\text{H}$  and  $^{13}\text{C}$  NMR; GC-MS; photodegradation

### СТУДИЈА ЗА ФОТОДЕГРАДАЦИЈА НА ИНСЕКТИЦИДОТ ФЕНВАЛЕРАТ СО $^1\text{H}$ NMR, $^{13}\text{C}$ NMR, И GC-MS И РАСВЕТЛУВАЊЕ НА СТРУКТУРАТА НА ПРОИЗВОДИТЕ НА ТРАНСФОРМАЦИЈА

Фотолизата на фенвалерат, пиретроиден инсектицид, беше следена во ацетонитрил со помош на  $^1\text{H}$  нуклеарна магнетна резонанција (NMR) и со  $^{13}\text{C}$  NMR, за да се идентификуваат

<sup>1</sup> Work presented at the 50th General Assembly & 47th International Union of Pure and Applied Chemistry (IUPAC) World Chemistry Congress (Abstract-P1047), 5–12 July 2019 in Paris, France. Theme 3: Chemistry for the Environment — Symposium 1: Monitoring Chemicals for a Safer Environment.

местата на кинење на хемиските врски како и со гасна хроматографија (GC-MS), за да се утврдат структурите на фотопродуктите на фенвалератот. UV-ирадијацијата на растворот на фенвалерат беше изведена со соларен симулатор во времетраење од 18 часа при што реакцијата на фотолиза следеше кинетика од прв ред. Вредностите на полувремето на живот ( $t_{1/2}$ ) се движеа помеѓу 15,25 и 21,63 h (удел на просечна фотодеградација = 51,7 %) за  $^1\text{H}$  NMR и меѓу 4,55 и 8,06 h (удел на просечна фотодеградација > 80 %) за  $^{13}\text{C}$  NMR. Беа забележани пет положби на раскинувањето на врските, карбонил-терцијарен јаглерод, терцијарен јаглерод-терцијарен јаглерод, карбонил-кислород, карбоксил-терцијарен јаглерод и ароматичен јаглерод-терцијарен јаглерод. За да се добие комплетен механизам на фотодеградацијата, беше применета GC-MS, како и  $^1\text{H}$  NMR и  $^{13}\text{C}$  NMR. Пред UV ирадијацијата беа добиени два пика што се должат на двата изомери на фенвалерат. При ирадијацијата, двата пика се намалуваат, а се појавуваат нови пикови што одговараат на образување на производи на фотодеградација. По 12 до 13 h, 99,39 % од фенвалератот беше разложено со просечна константа на брзината од  $0,305\text{ h}^{-1}$ . Хемиските структури на образуваните фотопроизводи беа идентификувани или со примена на спектралната база на податоци на NIST или со интерпретација на масените спектри. На крај беше предложен механизам на фотодеградација на фенвалератот.

**Клучни зборови:** фенвалерат; инсектицид;  $^1\text{H}$  и  $^{13}\text{C}$  NMR; GC-MS, фотодеградација

## 1. INTRODUCTION

When pesticides are spread into the environment, they undergo different types of physico-chemical processes, including transfers, immobilizations, and degradations. These processes reduce the number of active substances in the soil and decrease the pollution risk.<sup>1</sup> Furthermore, these processes can also lead to the dispersion of pesticides in food matrices, which can contribute to the poisoning of humans and animals.

Soil surface transfers account for only a small portion of applied pesticides, usually less than 5 %. These transfers contribute to the pollution of soil and surface or ground waters when pesticides are either dissolved or retained on ground particles. The transfers within soils are more important since pesticides are drained by rainwater and moved by water circulation.<sup>2</sup>

Immobilization processes of pesticides are mainly due to adsorption, resulting from the attraction of the active substances by mineral and organic constituents of soils, sediments, and surface and ground waters.<sup>2,3</sup>

Pesticide degradation in soil constitutes the main process which prevents the bioaccumulation of pollutants in the environment and depends on the specific physicochemical characteristics, such as pH values, organic matter, oxides, clays, etc.,<sup>4,5</sup> on the biological properties (microbiological species present in the media), and on the climatic conditions controlling ultraviolet (UV) irradiation, temperature, and soil moisture.<sup>1,6</sup> Thus, pesticide degradation can also take place by photochemistry,<sup>7-9</sup> as well as by electro-decomposition and thermal decomposition.<sup>10-12</sup> It is worthwhile to point out that, in some cases, the pesticide degradation products are more toxic than the native substances<sup>13</sup> and that pesticide molecules can

be degraded relatively rapidly in plants and soils according to the types of treatments and agronomic practices.<sup>14,15</sup>

Synthetic pyrethroids are like the natural pyrethrins and were widely used in agriculture and as household insecticides.<sup>16,17</sup> Consequently, their application in the environment can cause the pollution of soils and surface and ground waters.<sup>2</sup> Studies on the photochemical reactivity of pyrethroids, induced by natural or artificial light, have been carried out in organic or aqueous media and showed that these compounds were very light-sensitive.<sup>7,18</sup> The primary electronic excitation of pyrethroid molecules induced the formation, by bond cleavage, of numerous intermediates and unstable free radicals whose study was particularly useful, not only to understand the photodegradation mechanism, but also to identify the formed photoproducts.<sup>19,20</sup> In summary, when exposed to UV radiation, most pyrethroids exhibited photochemical reactions leading to photoproducts that could be analyzed by gas chromatography-mass spectrometry (GC-MS).

These pyrethroid insecticides were utilized in large amounts in Senegal, particularly in the Niayes agricultural area, where cultures are practiced during all seasons. Unfortunately, most of these insecticides presented a great photochemical instability and were rapidly degraded because of the very sunny, warm, and dry summer climate. In these conditions, it led to the formation of several toxic photoproducts.<sup>21</sup>

Therefore, we undertook the photodegradation study of fenvalerate, a pyrethroid insecticide widely used in agriculture in Senegal,<sup>22</sup> and we found that fenvalerate was photochemically transformed into more than twenty toxic breakdown products, which constituted an alarm signal on the

sanitary standpoint. Fenvalerate [4-chloro- $\alpha$ -(1-methylethyl) benzene acetic acid cyano(3-phenoxyphenyl)-methyl ester] possesses two stereogenic centers due to the presence of two asymmetrical carbon atoms and contains four stereoisomers of  $\alpha\text{S2R-}$ ,  $\alpha\text{R2S-}$ ,  $\alpha\text{R2R-}$ , and  $\alpha\text{S2S-}$  configurations.<sup>5</sup> It can cause severe toxicological effects in various aquatic organisms, especially in fish.<sup>23–25</sup> Also, after prenatal exposure in mice, fenvalerate was found to affect neurodevelopment in male offspring and fetal intrauterine growth restriction and exhibited enantio-selective toxicity on the earthworms.<sup>26–28</sup> Moreover, studies conducted on fenvalerate-exposed workers suggested that this insecticide or its transformation products induced morphologic abnormality and genotoxic defects of spermatozoa.<sup>29</sup>

In the present work, we investigated the fenvalerate photolysis by proton nuclear magnetic resonance ( $^1\text{H}$  NMR),  $^{13}\text{C}$  NMR, and GC-MS, using a solar light simulator as an irradiation source. Firstly, the kinetics of proton and carbon disappearance related to the observed variation of their chemical shifts were followed by  $^1\text{H}$  NMR and  $^{13}\text{C}$  NMR, respectively, which permitted us to determine the sites of bond cleavage and the formation of intermediate radicals. Secondly, GC-MS allowed us to monitor the fenvalerate photolysis and identify the photoproducts formed from the intermediate radicals. Finally, the combination of  $^1\text{H}$  NMR,  $^{13}\text{C}$  NMR, and GC-MS methods led us to propose a probable photodegradation mechanism of fenvalerate.

## 2. MATERIALS AND METHODS

### 2.1. Chemicals and reagents

Stock standard solutions of fenvalerate (420  $\mu\text{g ml}^{-1}$ ) were freshly prepared by dissolving the compound (99 %, PESTANAL<sup>®</sup>, analytical standard, Sigma-Aldrich, Saint Quentin Fallavier, France) in spectroscopic-grade solvents, including acetonitrile ( $\text{CH}_3\text{CN}$ ) and deuterated acetonitrile ( $\text{CD}_3\text{CN}$ ) obtained from Sigma Aldrich. We also verified that the old prepared solutions do not undergo any change before the measurement. These solutions were protected against light with aluminum foil and could be stored in a refrigerator at 6 °C for further use.

### 2.2. Photolysis reactions

Photolysis reactions were performed by irradiating a 25-ml volume of fenvalerate working solution introduced in a standard quartz three-mouth electrolytic tank (Xian Yima Optoelec Co., Ltd., China) with a LS1000 solar light simulator (Solar

Light Company, Inc.) for 18 hours at room temperature to achieve total degradation. For quality control, the blank solvents were analyzed before and after irradiation,  $\text{CD}_3\text{CN}$  in NMR and  $\text{CH}_3\text{CN}$  in GC-MS, and presented no impurities. On the other hand, the unirradiated parent product is by definition the reference.

Samples were taken every hour for analysis, and at nightfall, the solution was stored in the refrigerator at 6 °C in order to resume the next day. The NMR and GC-MS measurements was always done to check the stability before restarting irradiation. The solar light simulator single output produced an Air Mass 1.5 (AM 1.5) spectrum, which accurately replicated the full sunlight spectrum, with a sun output intensity and over 90% uniformity in the usable area.

The solar light simulator was equipped with a lamp (XPS-1000 Xenon Power Supply, Glenside, PA 19038, USA), and the power of the solar light simulator was set at 239  $\text{W/m}^2$ , corresponding approximately to the average annual solar radiation power in Senegal. The statistical analysis of data was performed with Origin Pro 8.5.1 (Origin Lab. Corporation, Northampton, MA 01060, USA) and Chem Draw<sup>®</sup> Ultra 8.0 (Cambridge Soft Corporation, 100 Cambridge Park Drive, Cambridge, MA 02140, USA).

### 2.3. NMR studies

Working solutions (58.8  $\mu\text{g mL}^{-1}$ ) were prepared by dissolving fenvalerate in  $\text{CD}_3\text{CN}$ . The photolysis reactions were performed by irradiating aliquots of the fenvalerate solution placed in a quartz tube. The NMR spectra were measured using a Nanobay NMR Avance III spectrometer of 400 MHz (9.4T) (Bruker Biospin GmbH, Rheinstetten, Germany) coupled to Topspin 3.1 software. It was equipped with a multinuclear z-gradient broad band fluorine observation (BBFO) Smart Probe (Bruker BioSpin Fällanden, Switzerland), allowing both direct and inverse detection of  $^1\text{H}$  and  $^{13}\text{C}$  in liquids. The pulse sequence was zg30 for  $^1\text{H}$  and zgpg30 for  $^{13}\text{C}$ , the number of scans was of 32 for  $^1\text{H}$  and 8,000 for  $^{13}\text{C}$ , and a tube diameter of 5 mm was used. All experiments were performed at room temperature (25 °C).

### 2.4. GC-MS analysis

Mass spectra and chromatograms were obtained using a Varian Ion Trap GC-MS. A GC with a split/splitless injector (Varian 431-GC, Agilent Technologies, Les Ulis, France) was coupled with a MS detector (Varian 210-MS, IT, Agilent Technologies, Santa Clara, CA 95051, USA). The

measurements were carried out under the following conditions: a volume of 2.0  $\mu\text{l}$  of fenvalerate solution ( $0.84 \text{ ng ml}^{-1}$ ), irradiated in  $\text{CH}_3\text{CN}$ , was injected in the splitless mode. A fused silica ZB-5MS capillary column ( $30 \text{ m} \times 0.25 \text{ mm} \times 0.25 \mu\text{m}$ ) from Phenomenex Zebron (Germany) was used by programming the column temperature variation from  $70 \text{ }^\circ\text{C}$  to  $175 \text{ }^\circ\text{C}$  at a rate of  $10 \text{ }^\circ\text{C}/\text{min}$ , then to  $225 \text{ }^\circ\text{C}$  at a rate of  $5 \text{ }^\circ\text{C}/\text{min}$ , and, finally, to  $310 \text{ }^\circ\text{C}$  at a rate of  $10 \text{ }^\circ\text{C}/\text{min}$  and held for 5 min. Helium (99.999 %) was used as carrier gas ( $1.0 \text{ mL}/\text{min}$ ). MS scanning conditions were as follows:  $m/z$  from 40 to 600, scan time = 0.5 s, electronic impact = 70 eV, and source temperature =  $300 \text{ }^\circ\text{C}$ . Varian MS Workstation version 6.9.1 (Agilent Technologies, Santa Clara, CAL, USA) enabled data acquisition in the single ion monitoring mode.

### 3. RESULTS AND DISCUSSION

#### 3.1. Study of fenvalerate photolysis by $^1\text{H}$ NMR in $\text{CD}_3\text{CN}$

The fenvalerate molecular structure, carrying the proton chemical shifts, evaluated with the Chem  $^1\text{H}$  NMR Estimation software is given in Figure 1, which served as a reference to identify the probable cleavage sites of bonds and photo-products formed during the fenvalerate photolysis under UV irradiation. We remember that  $^1\text{H}$  NMR spectroscopy was also applied by Yassine et al. (2018) to study the photodecomposition of novel oral anticoagulants dabigatran, rivaroxaban, and apixaban in different aqueous matrices.<sup>30</sup>

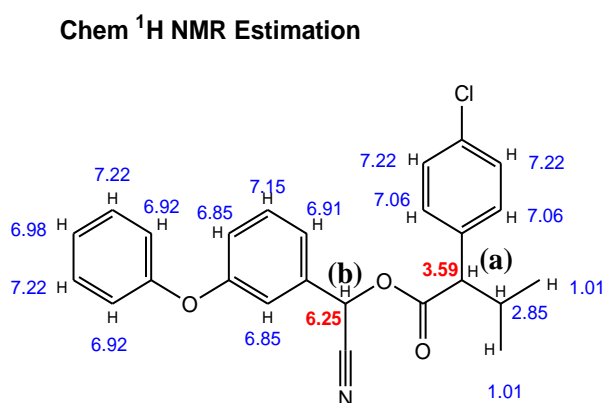


**Fig. 1.** Fenvalerate molecular structure, carrying the proton chemical shifts (in ppm), obtained with Chem  $^1\text{H}$  NMR Estimation Software

The  $^1\text{H}$  NMR spectra of fenvalerate in  $\text{CD}_3\text{CN}$  ( $\gamma = 58.8 \mu\text{g ml}^{-1}$ ), performed during its photolysis with the solar simulator (xenon lamp) at different irradiation times, are presented in Figure

2. Fenvalerate solutions were irradiated for 18 hours, and their irradiation produced important variations of proton signal intensity. During the UV irradiation, we observed a gradual disappearance of proton signal intensity at chemical shifts of 6.38, 6.35, 3.38, 3.34, 1.02, 0.95, and 0.68 ppm and a progressive increase of proton signal intensity at chemical shifts of 0.87, 1.09, and 1.15 ppm.

By comparing the proton chemical shifts ( $\delta$  in ppm) in Figures 1 and 2, we found that the  $\delta$  values observed at 3.38 and 3.34 ppm corresponded to the proton carried by carbon (a), whereas the proton  $\delta$  values located at 6.38 and 6.35 ppm were due to the proton of carbon (b). This clearly indicated that the chemical bond cleavage occurred on both carbons (a) and (b) bearing these protons, for which the NMR signal intensity decreased when the irradiation time increased. In all cases, the measurements were performed twice to ensure repeatability and reproducibility of the experiment.

The fenvalerate photolysis kinetics were investigated by following the proton intensity decrease at  $\delta = 6.38, 6.35, 3.38, 3.34, 1.02, 0.95,$  and  $0.68 \text{ ppm}$  with the irradiation time  $t$  (hour) in  $\text{CD}_3\text{CN}$ . In all cases, fenvalerate ( $58.8 \mu\text{g ml}^{-1}$ ) obeyed first-order kinetics, according to the equation:

$$\ln(f_0/f) = k_1 t \quad (1)$$

where  $f_0/f$  represents the ratio of the initial proton signal intensity at  $t_0 = 0$  to the proton signal intensity at an irradiation time  $t > t_0$ , and  $k_1$  is the first-order rate constant.

The  $k_1$  values were obtained by plotting  $\ln(f_0/f) = f(t)$ , and the half-life time ( $t_{1/2}$ ) values were determined from the following expression:

$$t_{1/2} = \ln(2/k_1) \quad (2)$$

The fenvalerate photodegradation kinetic parameters are given in Table 1 for all protons under study. As can be seen,  $k_1$  and  $t_{1/2}$  values were between  $3.20 \cdot 10^{-2}$  and  $4.55 \cdot 10^{-2} \text{ h}^{-1}$  and between 15.25 and 21.63 h, respectively, depending on the protons. After an 18-h irradiation, about half the intensity of the protons under study disappeared, with a photodegradation percentage (PP in %) value varying between 45 % and 56 % (mean photodegradation percentage = 51.7%), according to the protons (Table 1). The PP values were calculated by using the following equation:

$$PP = \left( \frac{f_0 - f}{f_0} \right) \times 100 \quad (3)$$

Similarly, Liu et al (2010) found that the fenvalerate and deltamethrin photodegradation processes in *n*-hexane and methanol/water (50/50 v/v) solutions also followed first-order kinetics.<sup>19</sup>

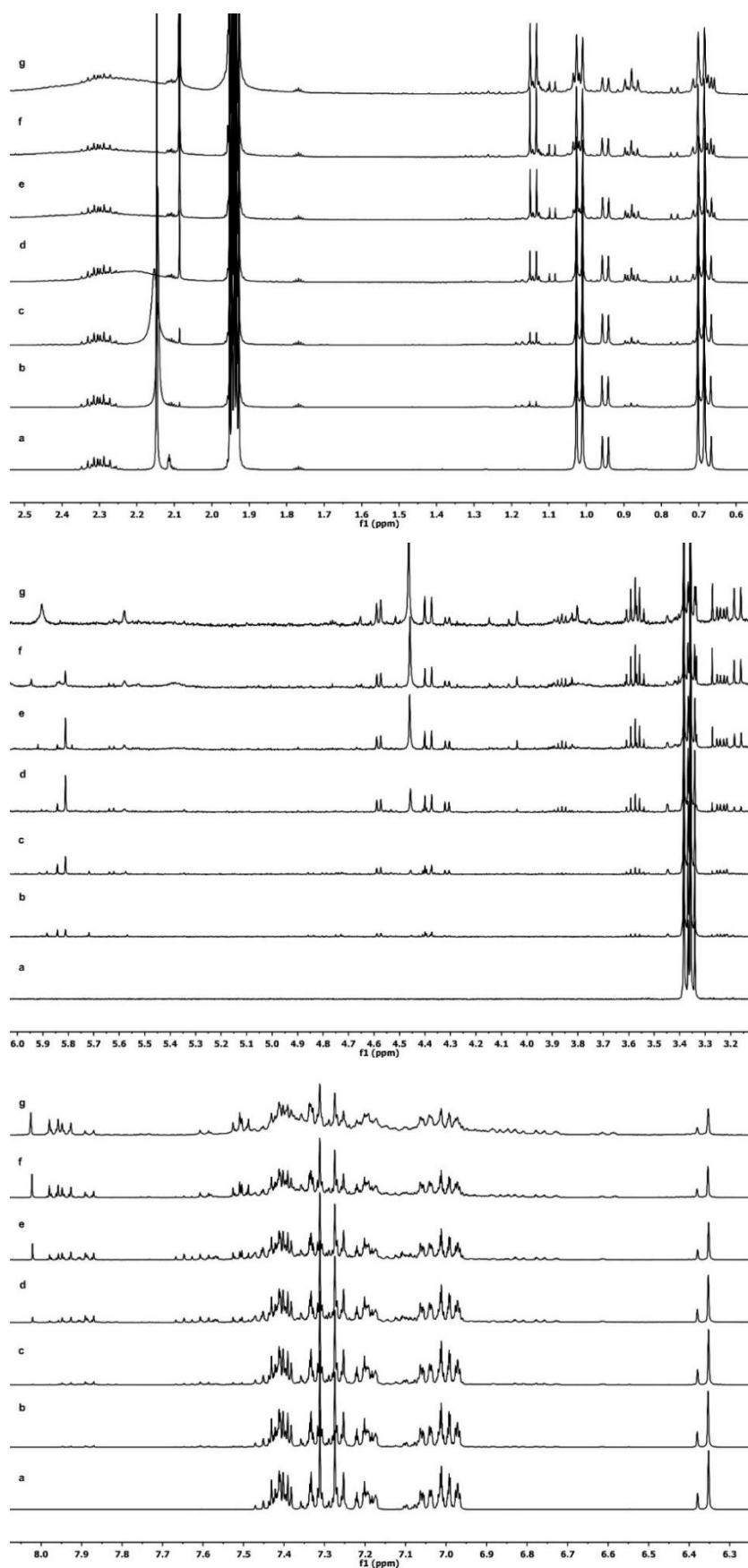


**Fig. 2.**  $^1\text{H}$  NMR spectra of fenvalerate, plotted as proton signal intensity (vertical axis, the scale unit is not available) vs. chemical shift  $\delta$  (in ppm, horizontal axis), obtained at different irradiation times  $t$  (a: 0, b: 1, c: 2, d: 6, e: 10, f: 14, and g: 18 h) in  $\text{CD}_3\text{CN}$ . Three  $^1\text{H}$  NMR spectra whose the chemical shift between 0.6 and 2.5 ppm; chemical shift between 3.2 and 6 ppm; chemical shift between 6.3 and 8 ppm were represented.

Table 1

Photodegradation kinetic parameters of fenvalerate, obtained in  $CD_3CN$  by  $^1H$  NMR and  $^{13}C$  NMR spectroscopy

Method	$\delta$ (ppm) <sup>a</sup>	$k_1$ ( $h^{-1}$ ) <sup>b</sup>	$t_{1/2}$ (h) <sup>c</sup>	PP (%) <sup>d</sup>	$r^2$ <sup>e</sup>
$^1H$ NMR	6.38	$4.35 (\pm 0.2) \cdot 10^{-2}$	15.93	54	0.998
	6.35	$4.55 (\pm 0.2) \cdot 10^{-2}$	15.25	56	0.998
	3.38	$3.74 (\pm 0.1) \cdot 10^{-2}$	18.54	50	0.998
	3.34	$3.20 (\pm 0.1) \cdot 10^{-2}$	21.63	45	0.998
	1.02	$3.87 (\pm 0.3) \cdot 10^{-2}$	17.92	52	0.996
	0.95	$3.95 (\pm 0.1) \cdot 10^{-2}$	17.55	52	0.997
	0.68	$4.08 (\pm 0.2) \cdot 10^{-2}$	16.98	53	0.997
$^{13}C$ NMR	32.3	$11.7 (\pm 0.9) \cdot 10^{-2}$	5.9	90	0.986
	63.0	$15.2 (\pm 1.4) \cdot 10^{-2}$	4.5	96	0.988
	64.0	$9.6 (\pm 0.7) \cdot 10^{-2}$	7.2	86	0.996
	172.5	$8.6 (\pm 0.9) \cdot 10^{-2}$	8.1	81	0.997

<sup>a</sup>  $\delta$  (ppm) = proton chemical shift or  $^{13}C$  chemical shift, <sup>b</sup>  $k_1$  = photolysis rate constant ( $h^{-1}$ ) and absolute error ( $\pm$ ), <sup>c</sup>  $t_{1/2}$  = photolysis half-life time (h), <sup>d</sup> PP (%) = photodegradation percentage, <sup>e</sup>  $r^2$  = correlation coefficient of the straight line

As already stated, this photolysis kinetic study of fenvalerate by  $^1H$  NMR demonstrated that the decrease of proton chemical shift intensity was due to the cleavage of C (a)-H and C (b)-H bonds (Figs. 1 and 2). Then, the observed variation in the rate and half-life values can be ascribed to the difference in rigidity of these chemical bonds.

Monitoring the fenvalerate photolysis under solar simulator irradiation by  $^1H$  NMR allowed us to determine four probable cleavage sites of bonds, leading to the photoproducts likely to be formed. The intermediate radicals (I, II, III, and IV) shown in Figure 3 yielded the initial photoproducts, which were expected to evolve towards other photoproducts.

To confirm these four cleavage sites, we also investigated the fenvalerate photolysis kinetics by  $^{13}C$  NMR spectroscopy under the same experimental conditions in the following section.

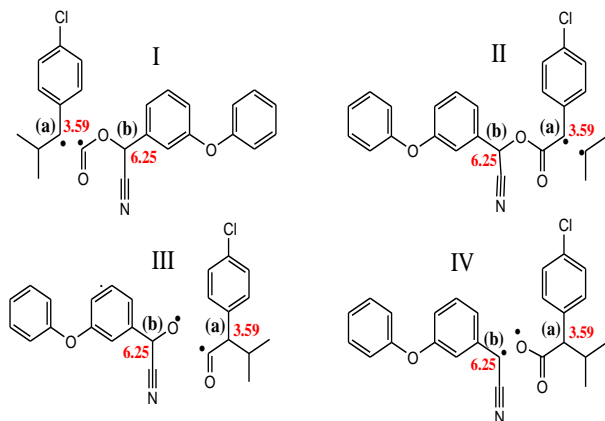


Fig. 3. Identification of radicals likely to be formed during the fenvalerate photolysis by  $^1H$  NMR

### 3.2. Study of fenvalerate photolysis by $^{13}C$ NMR in $CD_3CN$

A similar procedure was performed using  $^{13}C$  NMR spectroscopy. The fenvalerate molecular structure, carrying the carbon chemical shifts, evaluated with the Chem  $^{13}C$  NMR Estimation Software is presented in Figure 4. These carbon chemical shifts were compared with those obtained in our experimental  $^{13}C$  NMR spectroscopic study.

The  $^{13}C$  NMR spectra of fenvalerate in  $CD_3CN$  solutions ( $\gamma = 58.8 \mu g mL^{-1}$ ) were obtained at different UV irradiation times between 0 and 18 h. A progressive decrease in intensity of the carbon chemical shifts at 32.3, 63.0, 64.0, and 172.5 ppm were experimentally observed with the irradiation time. It is worthwhile to note that these experimental carbon chemical shift values are remarkably close to the calculated ones of Figure 4 ( $\delta = 32.1, 62.7, 63.1, \text{ and } 173.7$  ppm). Therefore, this decrease in intensity of carbon  $\delta$  values can be explained by the cleavage of bonds carried by these carbons.

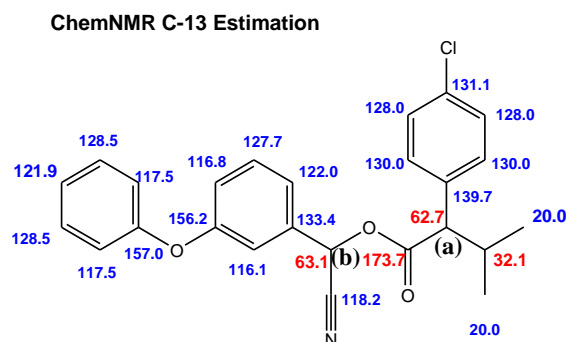


Fig. 4. Fenvalerate molecular structure, showing the carbon chemical shift values (in ppm), obtained with the Chem  $^{13}C$  NMR Estimation Software

Moreover, we noted the appearance of certain carbon  $\delta$  values ( $\delta = 19.0$  and  $31.0$  ppm) for which the intensity evolved during irradiation. This behavior might be explained by the transformation of the initial photoproducts into other photoproducts.<sup>32</sup>

The fenvalerate photolysis was investigated in  $\text{CD}_3\text{CN}$  by following the decrease of  $^{13}\text{C}$  intensity with the irradiation time (in hours) at  $\delta = 32.3$ ,  $63.0$ ,  $64.0$ , and  $172.5$  ppm. In all cases, the photolysis of fenvalerate ( $58.8 \mu\text{g ml}^{-1}$ ) obeyed first-order kinetics, according to equation (1). Like in the case of protons, we were able to determine the  $k_1$  (first-order rate constant) and  $t_{1/2}$  (half-life time) values from equations (1) and (2).

The fenvalerate photodegradation kinetic parameters are presented in Table 1 for all carbons under study. As can be seen,  $k_1$  and  $t_{1/2}$  values were between  $8.6 \cdot 10^{-2}$  and  $15.2 \cdot 10^{-2} \text{ h}^{-1}$  and  $4.5$  and  $8.1$  h, respectively, depending on the carbons. The rather small values of  $t_{1/2}$  and the fenvalerate PP values larger than  $80\%$  might explain the relatively rapid fenvalerate degradation under solar irradiation.

By examining the data in Table 1, it can be seen that the rate constants of the photodegradation reactions are a function of percentages of photodegradation. This observation helps to explain the differences in the values of  $k_1$  and  $t_{1/2}$  of the carbon and the proton, given that the experimental conditions were identical.

By comparing the calculated  $\delta$  values of Figure 4 to those obtained in our experimental  $^{13}\text{C}$  NMR spectroscopic study, it was possible to identify the  $^{13}\text{C}$  atoms for which the intensity decreased with irradiation time.

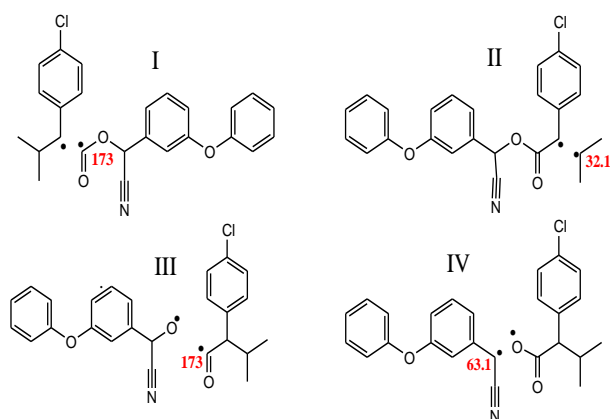


**Fig. 5.** Identification by of radicals likely to be formed during fenvalerate photolysis by  $^{13}\text{C}$  NMR

Therefore, we were able to determine four probable cleavage sites of the C-C bonds, which led to several radicals (Fig. 5), using  $^{13}\text{C}$  NMR spectroscopy. These cleavage sites (I–IV) were identical to those obtained by  $^1\text{H}$  NMR spectroscopy and led to the intermediate radicals given in Figure 5.

To provide a complete mechanism for the fenvalerate photodegradation, we complemented the  $^1\text{H}$  NMR and  $^{13}\text{C}$  NMR spectroscopic studies with GC-MS. The monitoring of fenvalerate photolysis by GC-MS allowed us to elucidate most of the formed photoproducts.

### 3.3. Study of fenvalerate photolysis by GC-MS in $\text{CH}_3\text{CN}$

The solar light simulator was used to follow the kinetics of fenvalerate photodegradation and photoproducts formation in  $\text{CH}_3\text{CN}$  by GC-MS. At  $t = 0$ , we observed two peaks of retention times  $t_R = 28.06$  and  $28.28$  min. These peaks corresponded to two of the four fenvalerate isomers as observed by Tagami et al. (2009), who determined fenvalerate residues in kampo products by GC-MS with negative chemical ionization.<sup>31</sup>

Solar light simulator irradiation of fenvalerate in  $\text{CH}_3\text{CN}$  led to the degradation of both fenvalerate isomer peaks and to the appearance of new, different peaks.

Among the different peaks, we chose to investigate the irradiation kinetics of both fenvalerate isomers and the first three formed photoproducts ( $t_R = 26.65$ ,  $27.00$ , and  $27.20$  min). We adopted the following notations:  $\text{F}_1$  ( $t_R = 28.06$  min) and  $\text{F}_2$  ( $t_R = 28.28$  min) correspond to the initial fenvalerate isomers ( $t = 0$ ), and  $\text{P}_1$  ( $t_R = 26.65$  min),  $\text{P}_2$  ( $t_R = 27.00$ ), and  $\text{P}_3$  ( $t_R = 27.20$ ) correspond to the first three photoproducts observed after UV irradiation.

Fenvalerate chromatograms obtained at various irradiation times ( $t = 0, 2, 5, 11, 15$ , and  $17$  h) in  $\text{CH}_3\text{CN}$  are presented in Figure 6. During the irradiation, we observed a significant and progressive decrease of the peak intensity for both fenvalerate isomers ( $\text{F}_1$  and  $\text{F}_2$ ). This indicated that fenvalerate was overly sensitive to sunlight. On the other hand, the intensity of  $\text{P}_1$ ,  $\text{P}_2$ , and  $\text{P}_3$  fenvalerate photoproducts increased during irradiation then progressively decreased (Fig. 6B–F). For more details on the variation of these photoproducts' concentrations during irradiation, see the section 3.3.1 related to Figure 8.

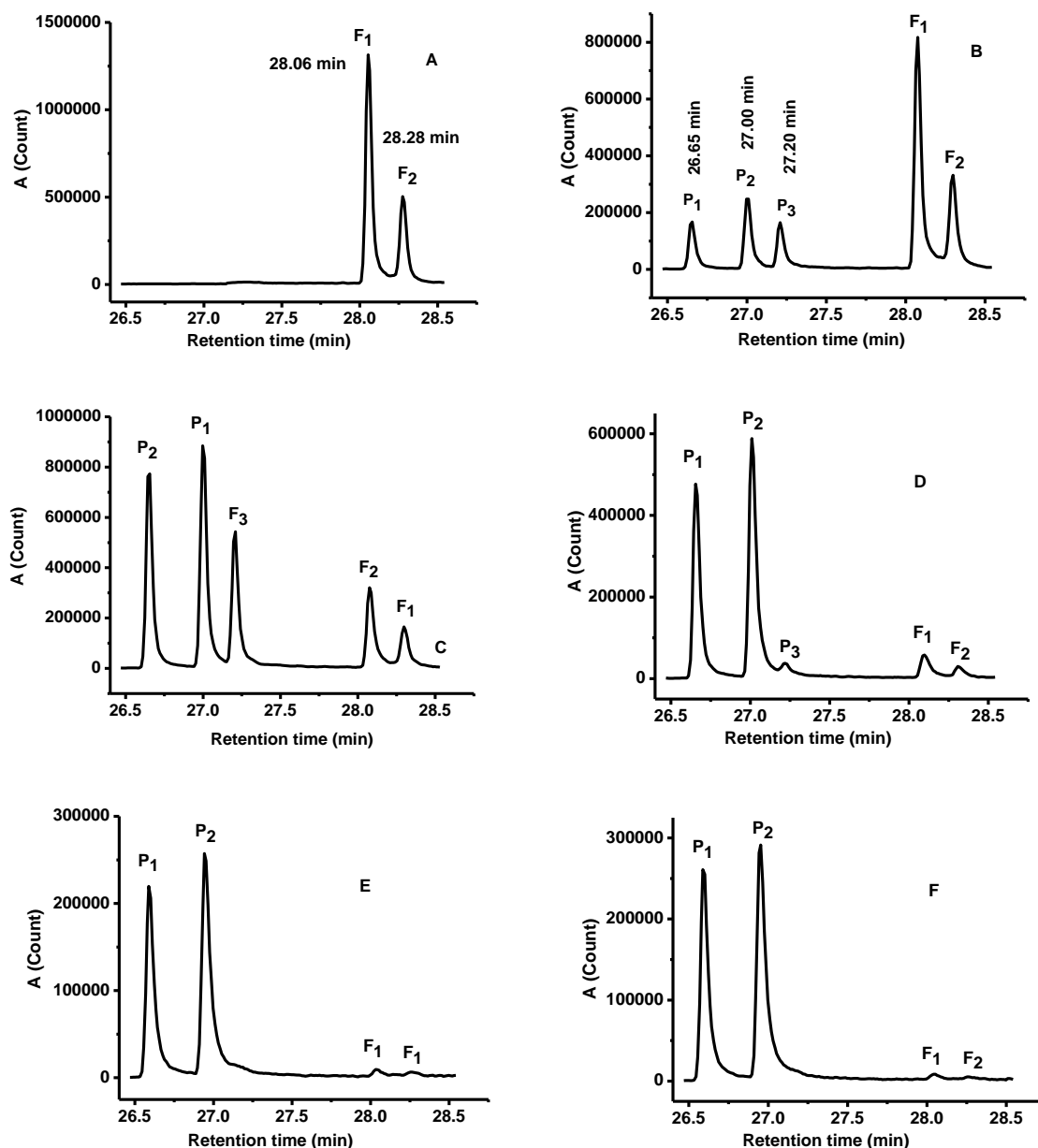


**Fig. 6.** Fenvalerate chromatograms at irradiation times: (A) 0 h, (B) 2 h, (C) 5 h, (D) 11 h, (E) 15 h, and (F) 17 h. F<sub>1</sub> and F<sub>2</sub> are the fenvalerate isomers; P<sub>1</sub>, P<sub>2</sub>, and P<sub>3</sub> are the first three photoproducts formed by irradiation

The photodegradation kinetics of fenvalerate isomers F<sub>1</sub> and F<sub>2</sub> are given in Figure 7. As can be seen, UV irradiation led to the progressive decrease of the chromatogram peaks of both isomers. In our experimental conditions, fenvalerate exponentially photodegraded with irradiation time; the exponential range ended at about 12 h, for which time the kinetic curves began to asymptotically trend to zero (Fig. 7). The photodegradation rate was found to follow first-order kinetics, since the plot of natural logarithm of % of F<sub>1</sub> or F<sub>2</sub> remaining concentration vs. the irradiation time yielded a linear relationship (inset of Fig. 7). Liu et al. (2010) also obtained first-order kinetics in their study of the photodegradation mechanism of del-

tamethrin and fenvalerate in simulated natural conditions.<sup>19</sup>

The results of fenvalerate photodegradation kinetics under solar light simulator irradiation are presented for both isomers in Table 2. The mean photolysis first-order rate constant ( $k_1$ ) and mean half-life time ( $t_{1/2}$ ) value of fenvalerate isomers were  $0.305 (\pm 0.02) \text{ h}^{-1}$  and  $2.28 (\pm 0.16) \text{ h}$ , respectively, which indicated that the fenvalerate photodegradation rate was relatively rapid. The correlation coefficient values of photodegradation kinetics were close to unity. Both isomers had similar  $k_1$  and  $t_{1/2}$  values, and their mean photodegradation percentage was practically 99.39 % for the 12- to 13-h irradiation times.

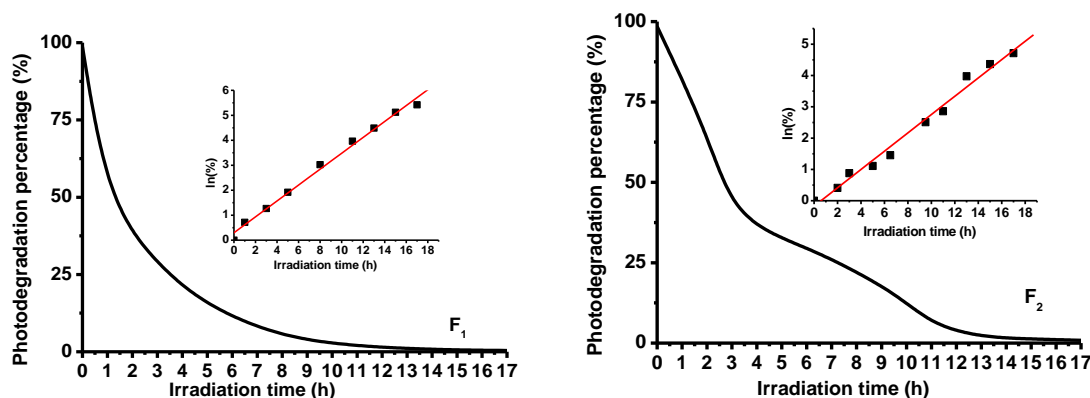


**Fig. 7.** Photodegradation kinetics of both fenvalerate isomers, F<sub>1</sub> and F<sub>2</sub>. Inset: ln (% of F<sub>1</sub> or F<sub>2</sub>) remaining concentration vs. irradiation time (in h)

Table 2

Photodegradation kinetic parameters of both fenvalerate isomers, obtained by GC-MS

Fenvalerate isomer	$k_1$ (h <sup>-1</sup> ) <sup>a</sup>	$t_{1/2}$ (h) <sup>b</sup>	PP (%) <sup>c</sup>	$r^2$ <sup>d</sup>
F <sub>1</sub> ( $t_R = 28.06$ min)	0.32 ( $\pm 0.07$ )	2.17	99.42	0.996
F <sub>2</sub> ( $t_R = 28.28$ min)	0.29 ( $\pm 0.05$ )	2.39	99.36	0.993

<sup>a</sup>  $k_1$  = photolysis rate constant (h<sup>-1</sup>) and absolute error ( $\pm$ ). <sup>b</sup>  $t_{1/2}$  = photolysis half-life time (h). <sup>c</sup> PP (%) = photodegradation percentage. <sup>d</sup>  $r^2$  = correlation coefficient

### 3.3.1. Photoformation and photodegradation of fenvalerate photoproducts

In Figure 8, we present the evolution of the first three fenvalerate photoproducts, including P<sub>1</sub>, P<sub>2</sub>, and P<sub>3</sub>, formed during fenvalerate solar light simulator irradiation in CH<sub>3</sub>CN. Two of the photoproducts, *i.e.*, P<sub>1</sub> and P<sub>2</sub>, exhibited the same behavior by evolving towards other photoproducts, as indicated in our previous photochemically-induced fluorescence (PIF) studies of fenvalerate in anionic micellar medium and in natural waters.<sup>7</sup> The fenvalerate enantiomers, F<sub>1</sub> and F<sub>2</sub>, were photodegraded and led to the photoformation of the three initial photoproducts, *i.e.*, P<sub>1</sub>, P<sub>2</sub>, and P<sub>3</sub>. Then, the first three photoproducts were phototransformed into other photoproducts when increasing the exposure time to the solar light simulator (Fig. 8). Therefore, it was observed that the first generated fenvalerate photoproducts were also sensitive to solar light. For all photoproducts, a kinetic profile showing a maximum value was obtained after a more or less long irradiation time, depending on the photoproduct.

The P<sub>3</sub> photoproduct was very rapidly photo-generated, reaching its maximum concentration after a relatively short exposure time (within 4–5 h) to the solar light simulator, then its complete photodegradation took place rapidly (Fig. 8, P<sub>3</sub> curve). In contrast, the P<sub>1</sub> and P<sub>2</sub> photoproducts were more slowly photogenerated, reaching a maximum concentration for a longer exposure time

(about 9–10 h), decreased rather rapidly, then remained at a quasi-constant concentration for irradiation times longer than 13 h (Fig. 8, curves of P<sub>1</sub> and P<sub>2</sub>). The presence of P<sub>1</sub> and P<sub>2</sub> photoproducts clearly demonstrated that fenvalerate did not persist in environmental matrices, but these potentially toxic photoproducts could be formed in natural waters and food matrices.

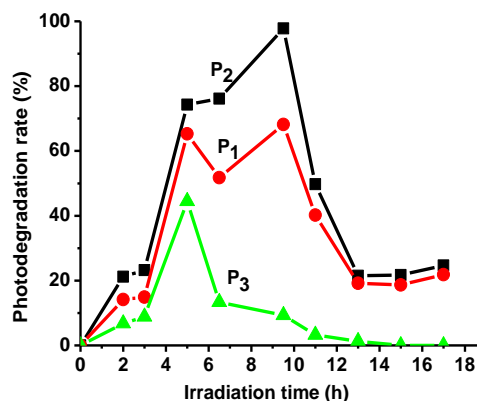


**Fig. 8.** Photoformation and photodegradation kinetics of the fenvalerate photoproducts P<sub>1</sub>, P<sub>2</sub>, and P<sub>3</sub> in CH<sub>3</sub>CN

### 3.3.2. Identification of fenvalerate photoproducts

As established in the previous section, exposure of fenvalerate to the solar light simulator led to the formation of a wide range of photoproducts.

These fenvalerate photoproducts were photodegraded and tentatively identified by means of their mass spectra (MS) or by using the NIST MS database (NIST 08, Software Version 2.0f, 2008;

Standard Reference Data Program). The identification of potential transformation products was based on the absence in blanks and controls, % NIST match, and retention time.

Table 3

*GC-MS detection and identification of fourteen photoproducts formed during fenvalerate photolysis, using the NIST MS database*

Photoproduct <sup>a</sup>	<i>t</i> <sub>R</sub> <sup>b</sup> (min)	Fragments ( <i>m/z</i> ) <sup>c</sup>	Structure <sup>d</sup>
(1) 1-Chloro-4-isobutyl benzene	13.25	125, 152, <u>168</u>	
(2) 4-Chlorophenyl-2-isopropyl-ethanal	27.00	108, <u>196</u>	
(3) 3-Phenoxybenzaldehyde	16.45	51, 141, <u>198</u>	
(4) 4-Phenoxybenzaldehyde	16.60	115, 141, <u>198</u> , 228	
(5) 3-Phenoxyphenyl acetonitrile	26.65	125, 127, <u>209</u>	
(6) 4-Phenoxyphenyl acetonitrile	26.74	125, 127, 207, <u>209</u>	
(7) 4-Chlorophenyl-2-isopropylethanoic acid	20.21	141, 167, <u>212</u>	
(8) 3-Phenoxybenzoic acid	19.75	115, 141, <u>214</u> , 225	
(9) 4-Phenoxybenzoic acid	19.81	115, 141, 198, <u>214</u>	
(10) Methyl-4-phenoxybenzoate	27.20	115, 141, 198, <u>252</u>	
(11) 3-Methyl-2-(4-(3-methyl-2-phenylbutanoyloxy)phenyl)butanoic acid	26.71	73, 221, <u>354</u> , <u>355</u>	
(12) Cyano(3-phenoxyphenyl)methyl 2-(4-chlorophenyl)acetate	27.22	75, 145, 225, 294, <u>377</u> , 429	

<sup>a</sup> Chemical name of the fenvalerate photoproducts. <sup>b</sup> *t*<sub>R</sub> = Photoproduct retention time (in min),

<sup>c</sup> Obtained MS fragments (*m/z*), the main fragment is underlined. <sup>d</sup> Chemical structure of the identified photoproducts

Twelve of the eighteen formed photoproducts were clearly identified. They are listed in Table 3 with their retention times, MS fragments, and chemical structures. In contrast, six other fenvalerate photoproducts were not found in the NIST MS database. Therefore, their identification was mainly based on MS interpretation and MS fragmentation pathways (Fig. 9A–D). By means of MS interpretation, it was possible to identify these photoproducts whose structures are summarized in Table 4.

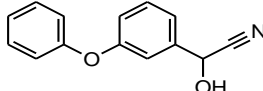
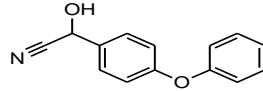
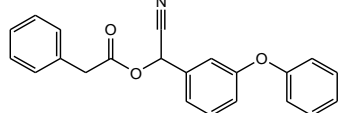
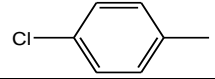
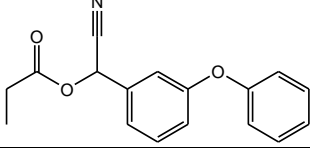
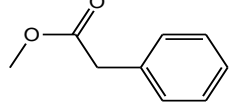
Comparing our work to literature data, we found that some fenvalerate photoproducts were already identified, such as: 1-chloro-4-isobutyl benzene, 3-phenoxybenzaldehyde, 4-phenoxybenzaldehyde, 3-phenoxyphenylacetonitrile, 4-phenoxyphenylacetonitrile, 3-phenoxybenzoic acid, and 4-phenoxybenzoic acid. Two cyanohydrin isomers were also found in the literature, cyano-3-phenoxyphenylmethanol<sup>19</sup> and cyano-4-phenoxyphenylmethanol.<sup>32</sup> Some of these fenvalerate photoproducts were determined in various studies, such as in *n*-hexane and methanol/water (50:50 V/V) by GC-MS,<sup>19</sup> in acetonitrile by UV/ozone-GC-MS,<sup>33</sup> by vacuum UV photoionization aerosol time-of-flight mass spectrometer (VUV-ATOF-

MS) and NMR and MS analysis,<sup>34</sup> and by Fourier-transform infrared spectroscopy (FTIR), followed by GC-MS.<sup>35</sup> Other authors investigated the fenvalerate photoproducts formed by biological degradation in soil using a bacterial strain, ZS-S-01,<sup>36</sup> by microbial degradation in surface soil with a native strain<sup>37</sup> and by photodegradation in *n*-hexane and methanol/water using GC-MS.<sup>38</sup> Also, Wang et al.<sup>34</sup> studied the chemical structure modification of fenvalerate after it had been metabolized in *Trichoplusia ni* (*Tn*) cells cultured in an insect medium, and treated with fenvalerate for 12 h and were able to identify the molecular metabolic basis of the insecticide's action inside the living cells. The analysis of the extracted degradation products by  $^1\text{H}$  NMR,  $^{13}\text{C}$  NMR, and mass spectrometry clearly showed the fenvalerate structure modification, which revealed the elimination of the  $\alpha$ -cyano group and the phenyl group of 3-phenoxybenzyl.<sup>34</sup>

All of these studies suggested that the fenvalerate photodegradation and biological degradation were based on four main reactions, including decyanation, photooxidation, ester cleavage, and photoisomerization.<sup>19,32–38</sup>

Table 4

GC-MS detection of other formed photoproducts, based on MS interpretation and on MS fragmentation pathways

Photoproduct	<i>m/z</i>	Structure
(13) Cyano-3-phenoxyphenylmethanol	225	
(14) Cyano-4-phenoxyphenylmethanol	225	
(15) Cyano(3-phenoxyphenyl)methyl 2-phenylacetate	343	
(16) 1-chloro-4-methylbenzene	126	
(17) Cyano(3-phenoxyphenyl)methyl propionate	281	
(18) Methyl 2-phenylacetate	150	

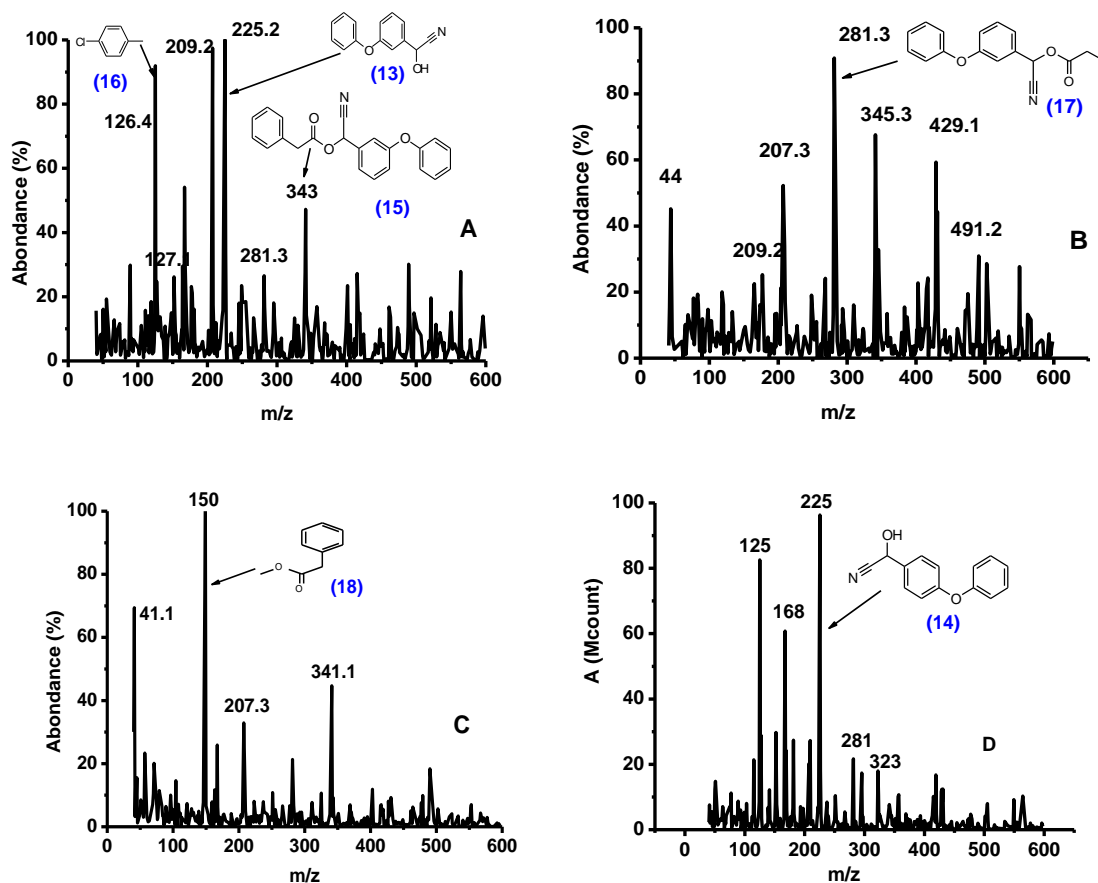


Fig. 9. Mass spectra fragmentation pathways of fenvalerate photolysis products in  $\text{CH}_3\text{CN}$

### 3.3.3. Proposition of a fenvalerate photodegradation mechanism

Our  $^1\text{H}$  NMR,  $^{13}\text{C}$  NMR, and GC-MS results on the fenvalerate photolysis allowed us to propose a photodegradation mechanism. An important issue related to the photodegradation of pesticides and other pollutants is the potential environmental risk factor associated with the toxicity of their degradation products and/or photoproducts. A tentative fenvalerate photodegradation mechanism is given in Figure 10.

The suggested reaction routes were built on the basis of the identified photoproducts, and four proposed tracks were presented as follows:

**Track I:** Photoproducts 1 and 10 were formed by homolytic cleavage of the carbonyl-tertiary carbon bond. Photoproduct 16 was obtained by removal of the isopropyl group from photoproduct 1, whereas photoproduct 17 resulted from different recombination reactions, including a process of tearing methyl groups from solvent molecules ( $\text{CH}_3\text{CN}$ ).

**Track II:** Photoproduct 12 was probably formed by homolytic cleavage of the tertiary carbon-tertiary carbon bond. Photoproduct 15, obtained from the removal of a chlorine atom from

photoproduct 12, was the result of secondary photoreactions. Thus, photoproduct 18 was obtained first by secondary photoreactions, then by removal of the methyl group from solvent molecules.

**Track III:** Photoproduct 2 and isomers 13 and 14 were probably formed by homolytic cleavage of the carbonyl-oxygen bond. Isomers 3 and 4 were obtained by decyanation (elimination of the CN group),<sup>19,33</sup> followed by a simple radical recombination or by dehydrocyanation (elimination of the HCN) from the isomers 13 and 14, respectively, whereas isomers 8 and 9 were obtained by photooxidation (oxidation of the carbonyl group to a carboxyl group) of isomers 3 and 4.

**Track IV:** Isomers 5 and 6 and photoproduct 7 were probably formed as a result of a homolytic cleavage of the carboxyl-tertiary carbon bond. Dimerization of photoproduct 7 yielded compound 11.

Although this study was not carried out under natural environmental conditions, it gives an idea of the diversity of the photodegradation products of the fenvalerate insecticide.

This study demonstrates that the photodegradation of fenvalerate does not only occur according to the four types of reactions described in the

literature (decyanation, photooxidation, ester cleavage, and photoisomerization); however, the proposed mechanism in this work allows us to observe the photoproducts formed by removal of the isopropyl group, removal of a chlorine atom, methylation, dehydrocyanation, and dimerization.

The results obtained here show that the degradation of a toxic pesticide under the effect of light can lead to the formation of other toxic byproducts. Moreover, our work clearly indicates that farmers and populations living in the Sahelian zone run a potential risk of poisoning linked to the photochemical degradation of pesticides in growing areas.

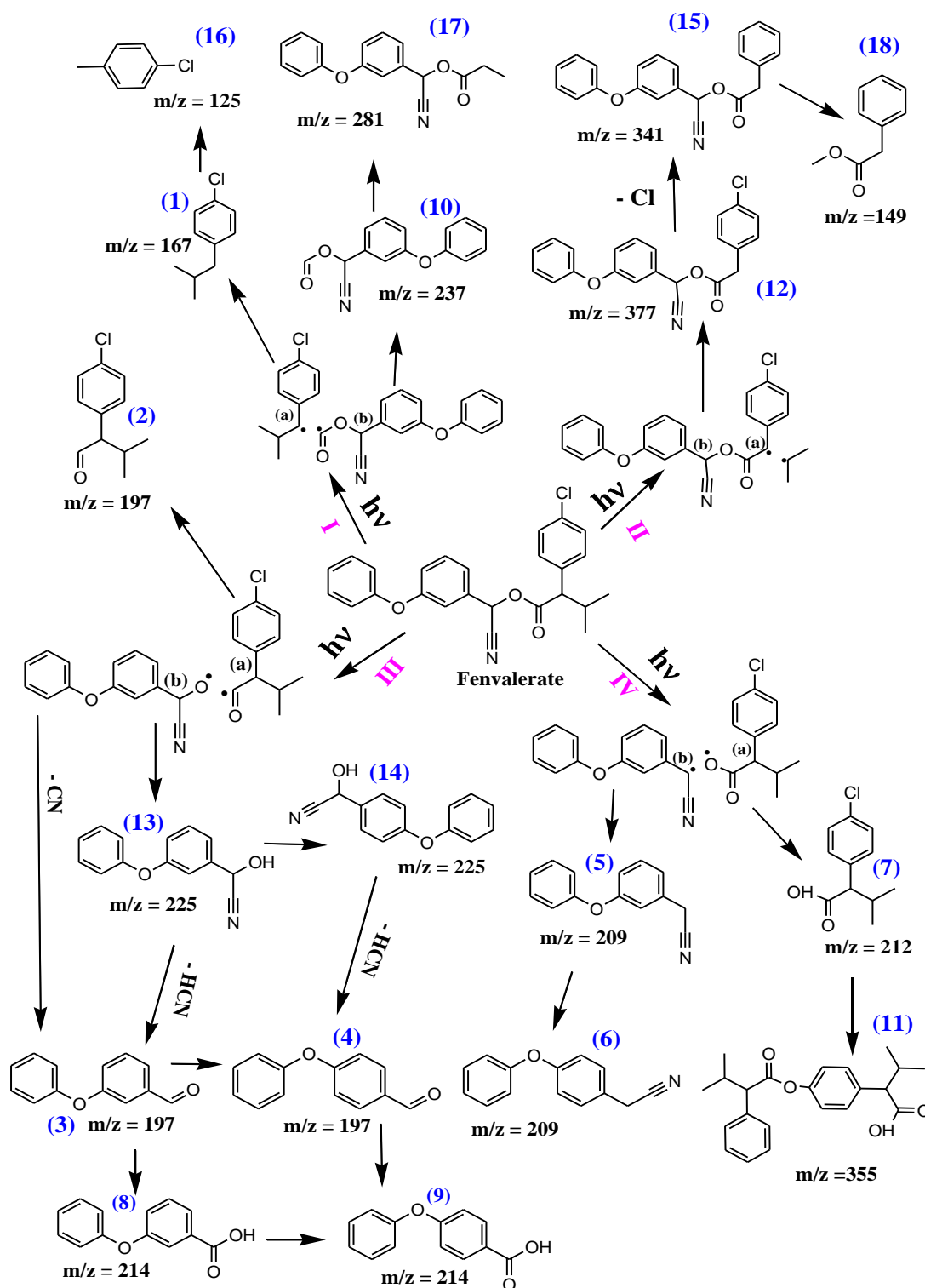


Fig. 10. Proposed fenvalerate photodegradation mechanism in  $\text{CH}_3\text{CN}$

## 4. CONCLUSION

Fenvalerate is a widely used insecticide that can be degraded into a number of photoproducts under the influence of sunlight. To establish the role and effects of these photoproducts, we studied the fenvalerate photolysis by  $^1\text{H}$  NMR,  $^{13}\text{C}$  NMR, and GC-MS to better understand the environmental fate of this insecticide. The combination of these three methods allowed us to establish the formation of eighteen fenvalerate photoproducts obtained under simulated sunlight irradiation and propose a probable mechanism for the photodegradation of this insecticide. Also, we were able to determine four homolytic cleavage sites, yielding the formation of intermediate radicals. Moreover, we formally identified twelve fenvalerate photoproducts using the NIST database and, afterwards, the other remaining photoproducts through mass spectra interpretation. The results of this work demonstrated the interest of combining the three methods to identify and possibly quantify the fenvalerate photoproducts formed under sunlight irradiation. In addition, these results should allow one to perform the analysis of fenvalerate and its metabolites in environmental matrices. In the future, we are planning to apply this combination of analytical methods for the determination of fenvalerate photoproducts in soil and natural water samples and to evaluate the toxicity of the various formed photoproducts, in order to improve the sanitary conditions of the agricultural use of this pesticide by farmers.

**Acknowledgements.** One of us, D.D. Thiaré, warmly thanks the Service of Cooperation and Cultural Action (SAC) of the French Embassy in Dakar (Senegal) for financial support of his research stay at the University of the Littoral Côte d'Opale (Dunkerque, France).

## REFERENCES

- (1) Mu, H.; Zhang, Z.; Yang, X.; Wang, K.; Xu, W.; Zhang, H.; Liu, X.; Ritsema, C. J.; Geissen V., Pesticide screening and health risk assessment of residential dust in a rural region of the North China Plain. *Chemosphere* **2022**, *303* (2), 135115. <https://doi.org/10.1016/j.chemosphere.2022.135115>
- (2) Affum, A. O.; Acquah, S. O.; Osae, S. D.; Kwaansa-Ansah, E. E., Distribution and risk assessment of banned and other current-use pesticides in surface and groundwaters consumed in an agricultural catchment dominated by cocoa crops in the Ankobra Basin, Ghana. *Sci. Total Environ.* **2018**, *633*, 630–640. <https://doi.org/10.1016/j.scitotenv.2018.03.129>
- (3) Cao, S.; Zhang, P.; Cai, M.; Yang, Y.; Liu, Y.; Ge, L.; Ma, H., Occurrence, spatial distributions, and ecological risk of pyrethroids in coastal regions of South Yellow and East China Seas. *Mar. Pollut. Bull.* **2022**, *179*, 113725. <https://doi.org/10.1016/j.marpolbul.2022.113725>
- (4) Sharma, M. V. P.; Kumari, V. D., Subrahmanyam, M., TiO<sub>2</sub> supported over SBA-15: on efficient photocatalyst for the pesticide degradation using solar light. *Chemosphere* **2008**, *73*, 1562–1569. <https://doi.org/10.1016/j.chemosphere.2008.07.081>
- (5) Li, Z.; Zhang, Z.; Zhang, L.; Leng, L., Isomer and enantioselective degradation and chiral stability of fenprothrin and fenvalerate in sols. *Chemosphere* **2009**, *76*, 509–516. <https://doi.org/10.1016/j.chemosphere.2009.03.015>
- (6) Bragança, I.; Mucha, A. P.; Tomasino, M. P.; Santos, F.; Lemos, P. C.; Delerue-Matos, C.; Domingues, V. P., Deltamethrin impact in a cabbage planted soil: Degradation and effect on microbial community structure. *Chemosphere* **2019**, *220*, 1179–1186. <https://doi.org/10.1016/j.chemosphere.2019.01.004>
- (7) Thiaré, D. D.; Coly, A.; Sarr, D.; Khonté, A.; Diop, A.; Gaye-Seye, M. D.; Delattre, F.; Tine, A.; Aaron, J. J., Determination of the fenvalerate insecticide in natural waters by a photochemically-induced fluorescence method. *Maced. J. Chem. Chem. Eng.* **2015**, *34*, 245–254. <https://dx.doi.org/10.20450/mjce.2015.726>
- (8) Bakhoun, J. P.; Mbaye, O. M. A.; Diaw, P. A.; Mbaye, M.; Cissé, L.; Gaye-Seye, M. D.; Aaron, J. J.; Coly, A.; Le Jeune, B.; Giamarchi, P., Ultraviolet photo-induced fluorescence followed by laser excitation (UV-PIF-LE) for the determination of pesticides in natural waters. *Anal. Lett.* **2019**, *52*, 2782–2793. <https://doi.org/10.1000/00032719.2019.1604724>
- (9) Saleck, M. L. O.; Thiaré, D. D.; Sambou, S.; Bodian, E. H. T.; Sarr, I.; Sarr, D.; Diop, C.; Gaye-Seye, M. D.; Fall, M.; Coly, A., Photochemically-induced fluorescence (PIF) and UV-VIS absorption determination of diuron and metalaxyl in well water, kinetic of photodegradation and rate of leach ability in soils. *Anal. Chem. Lett.* **2019**, *9*, 806–815. <https://doi.org/10.1080/22297928.2020.1712237>
- (10) Diaw, P. A.; Oturan, N.; Gaye-Seye, M. D.; Mbaye, O. M. A.; Mbaye, M.; Coly, A.; Aaron, J. J.; Oturan, M. A., Removal of the herbicide monolinuron from waters by the electro-Fenton treatment. *J. Electroanal. Chem.* **2020**, *864*, 114087. <https://doi.org/10.1016/j.jelechem.2020.114087>
- (11) Fdez-Sanromán, A.; Acevedo-García, V.; Pazos, M.; Sanromán, M. Á.; Rosales, E., Iron-doped cathodes for electro-fenton implementation: application for pymetrozine degradation. *Electrochim. Acta* **2020**, *338*, 135768. <https://doi.org/10.1016/j.electacta.2020.135768>
- (12) Mendy, A.; Thiaré, D. D.; Sambou, S.; Khonté, A.; Coly, A.; Gaye-Seye, M. D.; Delattre, F.; Tine, A., New method for the determination of metolachlor and butprofazin in natural water using orthophthalaldehyde by thermochemically-induced fluorescence derivatization (TIFD). *Talanta* **2016**, *151*, 202–208. <https://dx.doi.org/10.1016/j.talanta.2016.01.036>
- (13) Sud, D.; Kumar, J.; Kaur, P.; Bansal, P., Toxicity, natural and induced degradation of chlorpyrifos. *J. Chil. Chem. Soc.* **2020**, *65*, 4807–4816. <http://dx.doi.org/10.4067/S0717-97072020000204807>

- (14) Juraske, R.; Castells, F.; Vijay, A.; Muñoz, P.; Antón, A., Uptake and persistence of pesticides in plants: Measurements and model estimates for imidacloprid after foliar and soil application. *J. Hazard. Mater.* **2009**, *165*, 683–689. <https://doi.org/10.1016/j.jhazmat.2008.10.043>
- (15) Castro-Gutierrez, V. M.; Hassard, F.; Moir, J. W. B., Probe-based qPCR assay enables the rapid and specific detection of bacterial degrading genes for the pesticide metaldehyde in soil. *J. Microbiol. Methods* **2022**, *195*, 106447. <https://doi.org/10.1016/j.mimet.2022.106447>
- (16) Bibbs, C. S.; Kaufman, P. E., Volatile Pyrethroids as a potential mosquito abatement tool: A review of pyrethroid-containing spatial repellents. *J. Integr. Pest. Manag.* **2017**, *8*, 1–10. <https://doi.org/10.1093/jipm/pmx016>
- (17) Buhagiar, T. S.; Devine, G. J.; Ritchie, S. A., Metofluthrin: investigations into the use of a volatile spatial pyrethroid in a global spread of dengue, chikungunya and Zika viruses, *Parasit. Vectors* **2017**, *10*, 1–12. <https://doi.org/10.1186/s13071-017-2219-0>
- (18) Possetto, D.; Reynoso, A.; Natera, J.; Massad, W. A., Kinetics of the riboflavin-sensitized degradation of pyrethroid insecticides. *J. Photochem. Photobiol. A* **2021**, *418*, 113416. <https://doi.org/10.1016/j.jphotochem.2021.113416>
- (19) Liu, P., Liu, Y., Liu, Q.; Liu, J., Photodegradation mechanism of deltamethrin and fenvalerate. *J. Environ. Sci.* **2010**, *22*, 1123–1128. [https://doi.org/10.1016/S1001-0742\(09\)60227-8](https://doi.org/10.1016/S1001-0742(09)60227-8)
- (20) Diaw, P. A.; Mbaye, O. M. A.; Thiaré, D. D.; Oturan, N. B.; Gaye-Seye, M. D.; Coly, A.; Le Jeune, B.; Giamarchi, P.; Oturan, M. A.; Aaron, J. J.; Combination of photoinduced fluorescence and GC-MS for elucidating the photodegradation mechanisms of diflufenzuron and fenuron pesticides. *Luminescence* **2019**, *34*, 465–471. <https://doi.org/10.1002/bio.3612>
- (21) Diop, A., *Diagnosis of use practices and quantification of pesticides in the Niayes zone of Dakar (Senegal)*. Thesis of Doctorate, Université du Littoral Côte d'Opale, France, 2013, (NNT: 2013 DUNK 0341).
- (22) Diop, A.; Diop, Y. M.; Thiaré, D. D.; Cazier, F.; Sarr, S. O.; Kasprowiak, A.; Landy, D.; Delattre, F., Monitoring survey of the use patterns and pesticide residues on vegetables in the Niayes zone, Senegal. *Chemosphere* **2016**, *144*, 1715–1721. <https://doi.org/10.1016/j.chemosphere.2015.10.058>
- (23) Zhang, Q.; Zhang, Y.; Du, J.; Zhao, M., Environmentally relevant levels of  $\lambda$ -cyhalothrin, fenvalerate, and permethrin cause developmental toxicity and disrupt endocrine system in zebrafish (*Danio rerio*) embryo. *Chemosphere* **2017**, *185*, 1173–1180. <https://doi.org/10.1016/j.chemosphere.2017.07.091>
- (24) Zhang, L.; Hong, X.; Yan, S.; Zha, J., Environmentally relevant concentrations of fenvalerate induces immunotoxicity and reduces pathogen resistance in Chinese rare minnow (*Gobiocypris rarus*). *Sci. Total Environ.* **2022**, *838*, 156347. <https://doi.org/10.1016/j.scitotenv.2022.156347>
- (25) Mahmouda, A. H.; Darwish, N. M.; Kim, Y. O.; Viayaraghavan, P.; Kwon, J.; Na, S. W.; Lee, J. C.; Kim, H., Fenvalerate induced toxicity in Zebra fish, *Danio rerio* and analysis of biochemical changes and insights of digestive enzymes as important markers in risk assessment. *J. King Saud. Univ. Sci.* **2020**, *32*, 1569–1580. <https://doi.org/10.1016/j.jksus.2019.12.013>
- (26) Guo, C.; Yang, Y.; Shi, M. X.; Wang, B.; Liu, J. J.; Xu, D. X.; Meng, X. H., Critical time window of fenvalerate-induced fetal intrauterine growth restriction in mice. *Ecotox. Environ. Saf.* **2019**, *172*, 186–193. <https://doi.org/10.1016/j.ecoenv.2019.01.054>
- (27) Zhang, H.; Lu, T.; Feng, Y.; Sun, X.; Yang, X.; Zhou, K.; Sun, R.; Wang, Y.; Wang, X.; Chen, M., A metabolomic study on the gender-dependent effects of maternal exposure to fenvalerate on neurodevelopment in offspring mice. *Sci. Total Environ.* **2020**, *707*, 136130. <https://doi.org/10.1016/j.scitotenv.2019.136130>
- (28) Ye, X.; Xiong, K.; Liu, J., Comparative toxicity and bioaccumulation of fenvalerate and esfenvalerate to earthworm *Eisenia fetida*. *J. Hazard. Mater.* **2016**, *5*, 82–88. <https://doi.org/10.1016/j.jhazmat.2016.02.010>
- (29) Xia, Y.; Bian, Q.; Xu, L.; Cheng, S.; Song, L.; Liu, J.; Wu, W.; Wang, S.; Wang, X.; Genotoxic effects on human spermatozoa among pesticide factory workers exposed to fenvalerate, *Toxicology* **2004**, *203*, 49–60. <https://doi.org/10.1016/j.tox.2004.05.018>
- (30) Yassine, M.; Fuster, L.; Dévier, M. H.; Geneste, E.; Pardon, P.; Grélard, A.; Dufourc, E.; Iskandarani, M. A.; Aït-Aïssa, S.; Garric, J.; Budzinski, H.; Mazellier, P.; Trivella, A. S., Photodegradation of novel oral anticoagulants under sunlight irradiation in aqueous matrices, *Chemosphere* **2018**, *193*, 329–336. <https://doi.org/10.1016/j.chemosphere.2017.11.036>
- (31) Tagami, T.; Kajimura, K.; Yamasaki, K.; Sawabe, Y.; Nomura, C.; Taguchi, S.; Obana, H., Simple and rapid determination of cypermethrin and fenvalerate residues in Kampo products by gas chromatography-mass spectrometry with negative chemical ionization. *J. Health Sci.* **2009**, *55*, 777–782. <https://doi.org/10.1248/jhs.55.777>
- (32) Raikwar, M. K.; Nag, S. K., Phototransformation of alphacypermethrin as thin film on glass and soil surface. *J Environ Sci Health - B Pestic Food Contam Agric Wastes* **2014**, *41*, 973–988. <http://dx.doi.org/10.1080/03601230600806186>
- (33) Tran, N. T. T.; Trinh, T. H.; Hoang, N. M.; Ngo, T. M., UV/ozone Treatment of the pyrethroid insecticide fenvalerate in aqueous solutions, *APCBEE Procedia* **2014**, *8*, 151–155. <https://dx.doi.org/10.1016/j.apcbee.2014.03.018>
- (34) Wang, Z.; Xu, W.; Zhao, X.; Fang, P.; Wang, L.; Qiao, Z., Structure modification of fenvalerate metabolized in *Trichoplusia ni* cells. *Acta Biochim. Biophys. Sin.* **2013**, *45*: 792–794. <https://doi.org/10.1093/abbs/gmt068>
- (35) Segal-Rosenheimer, M.; Dubowski, Y., Photolysis of thin films of cypermethrin using in situ FTIR monitoring: Products, rates and quantum yields. *J. Photochem. Photobiol. A* **2008**, *200*, 262–269. <https://doi.org/10.1016/j.jphotochem.2008.08.004>
- (36) Chen, S.; Yang, L.; Hu, M.; Liu, J., Biodegradation of fenvalerate and 3-phenoxybenzoic acid by a novel *Stenotrophomonas* sp. strain ZS-S-01 and its use in

- bioremediation of contaminated soils. *Appl. Microbiol. Biotechnol.* **2011**, *90*, 755–767.  
<https://doi.org/10.1007/s00253-010-3035-z>
- (37) Massiha, A.; Pahlaviani, M. R. M. K.; Issazadeh, K., Microbial degradation of pesticides in surface soil using native strain in Iran, *International Conference on Bio-technology and Environment Management (IPCBEE)*, Singapore **2011**, *18*, 76–81.
- (38) Nahri-Niknafs, B.; Ahmadi, A., Photodegradation of deltamethrin and fenvalerate under simulated solar light irradiation and identification of photoproduct. *Rev. Chim.* **2013**, *64*, 828–831.